# Integration of satellite and in situ data to measure $CO_2$ fluxes in the Mediterranean Sea

# Outline:

- Carbon cycle
- Objectives
- In situ $pCO_2$ and $CO_2$ fluxes
- Satellite algorithms
- Results and discussion
- Conclusions and next steps

# Outline:

- **Carbon cycle**
- Objectives
- In situ $pCO_2$ and $CO_2$ fluxes
- Satellite algorithms
- Results and discussion
- Conclusions and next steps

# Carbon cycle – brief overview

Atmospheric $CO_2$ concentration increased from about 280 ppm in pre-industrial times to the actual value of about 420 ppm due to antropogenic activities

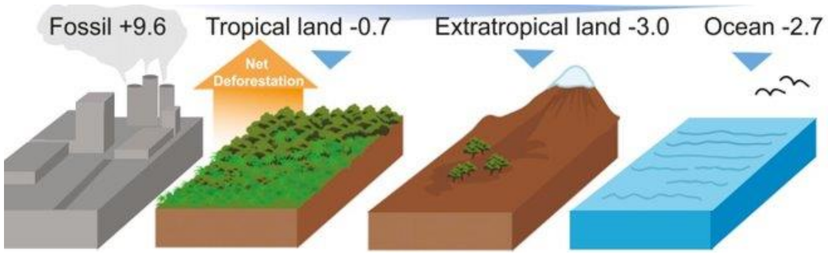


**Atmospheric increase 4.7 Pg/y**

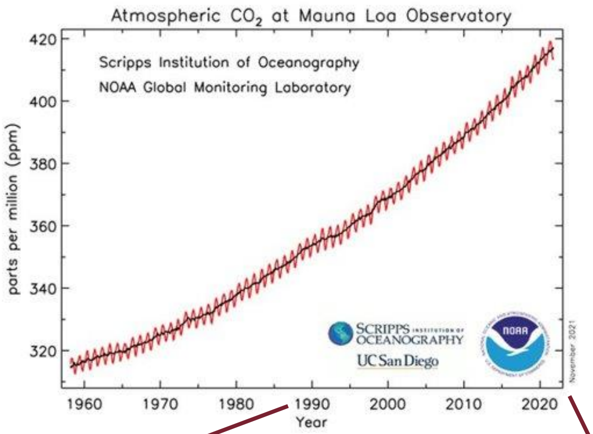


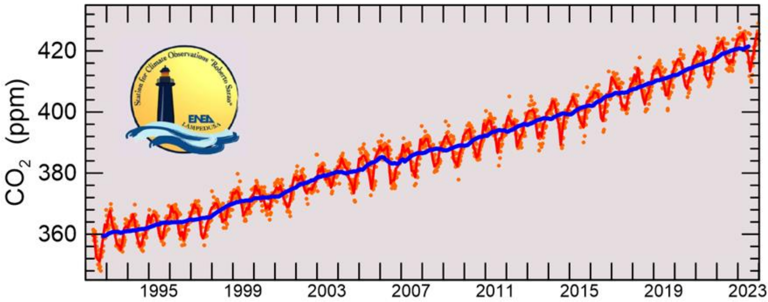


Sellers, P. J. et al., Observing carbon cycle–climate feedbacks from space. *Proceedings of the National Academy of Sciences of the United States of America*. National Academy of Sciences. https://doi.org/10.1073pnas.1716613115, 2018

# Carbon cycle – brief overview

- Ocean interaction with $CO_2$ has a great spatio-temporal variability not fully characterised with complex dependencies on phisycal, biological and chemical properties of the ocean

- $CO_2$ absorption leads to the acidification of ocean waters which can trigger negative feedbacks on absorption efficency

- Climate feedbacks are unknown

- Lack of continuous in situ measurements

- Ocean $CO_2$ absorption efficiency is strongly related with climate evolution

**Monitoring atmosphere-ocean exchanges is crucial**

# Carbon cycle – ocean-atmosphere fluxes

$$\boxed{\mathbf{F = K_{wa}\,KH\,(\Delta pCO_2)_{sea\text{-}atm}}}$$

- $K_{wa} = 0.251 <U^2> (Sc/660)^{-0.5}$ is the Gas Transfer Velocity
- $Sc = A + B*SST + C*SST^2 + D*SST^3 + E*SST^4$ is the Schmidt Number
- $\ln(KH) = A_1 + A_2*(100/SST) + A_3*\ln(SST/100) + SSS*[B_1 + B_2*(SST/100) + B_3*(SST/100)^2]$ is the gas solubility
- Sea $pCO_2$ can be measured or derived
- Air $pCO_2$ can be measured or derived

Wanninkhof, R., Relationship between wind speed and gas exchange over the ocean revisited, *Limnol. Oceanogr. Methods*, 12, doi:10.4319/lom.2014.12.351, 2014

# Marine carbon cycle

- Current monitoring mainly rely on model-based estimates of $pCO_2$ and $CO_2$ fluxes

- Works on satellite-based estimates of $pCO_2$

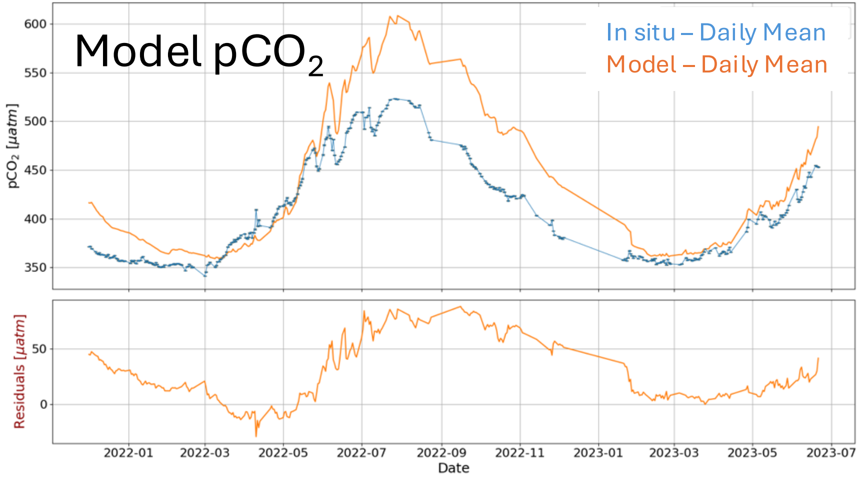


Mediterranean Sea Biogeochemistry Analysis and Forecast - https://doi.org/10.25423/cmcc/medsea_analysisforecast_bgc_006_014_medbfm3

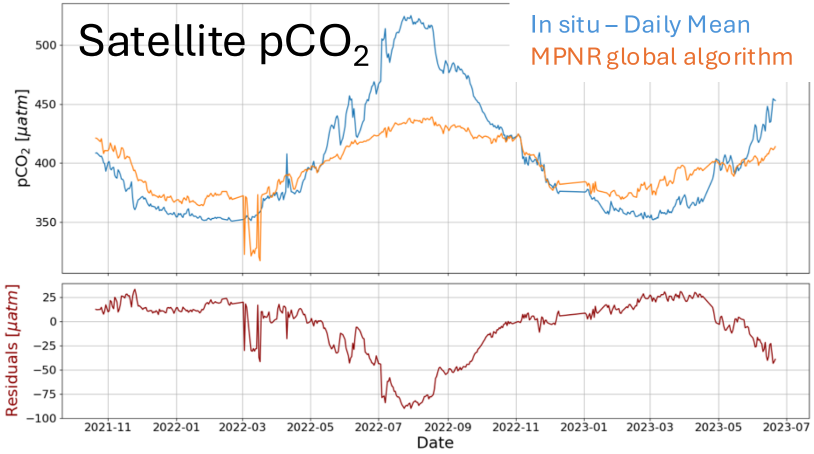


K. V. Krishna, P. Shanmugam and P. V. Nagamani, "A Multiparametric Nonlinear Regression Approach for the Estimation of Global Surface Ocean pCO2 Using Satellite Oceanographic Data," in *IEEE Journal of Selected Topics in Applied Earth Observations and Remote Sensing*, vol. 13, pp. 6220-6235, 2020, doi: 10.1109/JSTARS.2020.3026363.

# Marine carbon cycle

- Current monitoring mainly rely on model-based estimates of $pCO_2$ and $CO_2$ fluxes
- Works on satellite-based estimates of $pCO_2$
- Sparse in situ continuos and naval occasional measurements
- Carbon global monitoring projects and datasets:
  - Global carbon budget (https://www.globalcarbonproject.org/)
  - Surface Ocean $CO_2$ atlas (https://socat.info/)

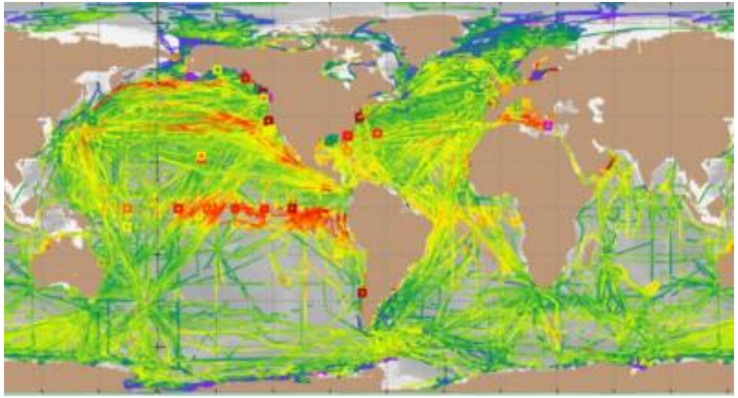

# Marine carbon cycle

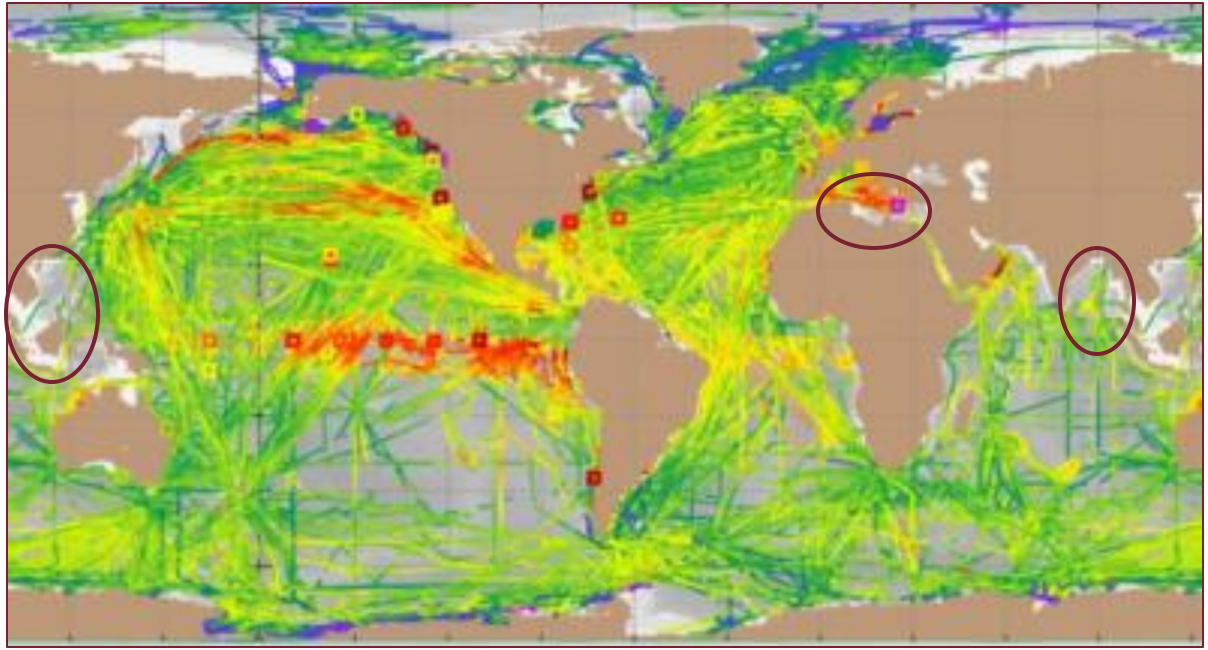

Still missing estimates, including large portion of marginal seas

K. Lee, C.L. Sabine, T. Tanhua, T.W. Kim, R.A. Feely, and H.C. Kim. Roles of marginal seas in absorbing and storing fossil fuel CO2. Energy & Environmental Science, 4:1133–1146, 2011. doi: https://doi.org/10.1039/C0EE00663G.

# Outline:

- Carbon cycle
- **Objectives**
- In situ $pCO_2$ and $CO_2$ fluxes
- Satellite algorithms
- Results and discussion
- Conclusions and next steps

# Thesis objectives

- Characterization of the Central Mediterranean carbon cycle using in situ data
- Satellite $pCO_2$ estimates using proxies for spatial monitoring
- $CO_2$ fluxes estimates merging satellite, model and in situ data

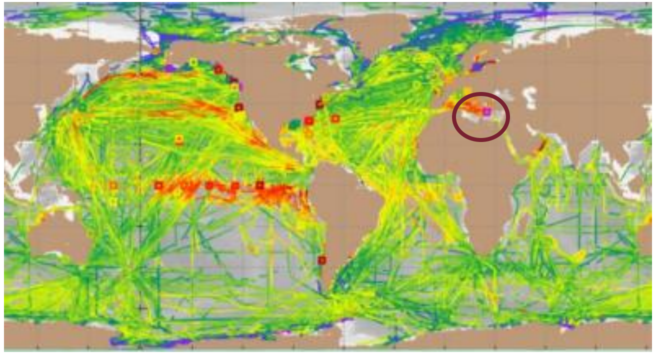

# Outline:

- Carbon cycle
- Objectives
- **In situ $pCO_2$ and $CO_2$ fluxes**
- Satellite algorithms
- Results and discussion
- Conclusions and next steps

# Mediterranean Sea

- Climate hotspot
- Semi-enclosed basin under environmental stress
- Few carbon in situ measurements
- Few studies on basin-wide carbon cycle
- Suffering long and intense marine heatwaves (2022-2023; 2023-2024)

Marullo, S., Serva, F., Iacono, R., Napolitano, E., di Sarra, A., Meloni, D., . . . Santoleri, R. (2023). Record-breaking persistence of the 2022/23 marine heatwave in the Mediterranean Sea. Environmental Research Letters, 18 (11), 114041. https://doi.org/10.1088/1748-9326/ad02ae

# Study site

In situ measurements made at **Lampedusa**

- Small island with small pollution sources
- Far from land
- Representative for background conditions
- Host observatories (AO, OO, EO) for climate studies and carbon monitoring (within the Integrated Carbon Observation System - **ICOS infrastructure**)

- Ocean $pCO_2$, temperature and salinity are available at 5 m depth from October 2021 at OO
- Wind speed, atmospheric pressure, atmospheric $CO_2$ concentration are available at AO

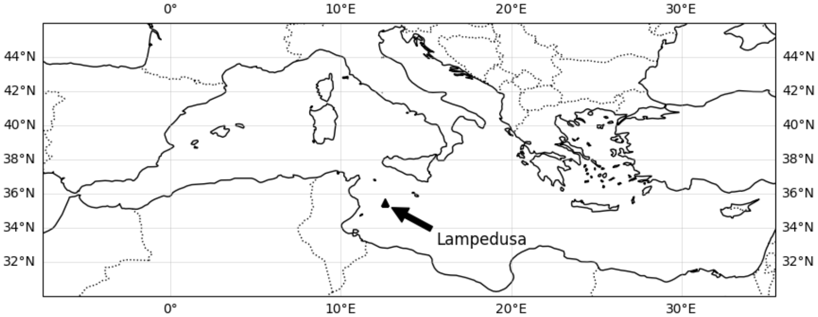


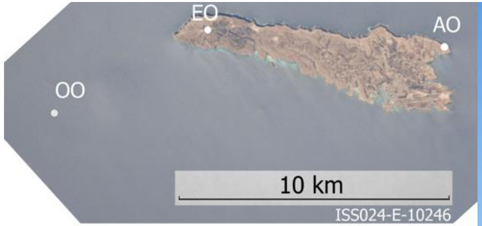


# Study site

In situ measurements made at **Lampedusa**

- Small island with small pollution sources
- Far from land
- Representative for background conditions
- Host observatories (AO, OO, EO) for climate studies and carbon monitoring

| Variable | Instrument | Accuracy | Height (asl) |
|---|---|---|---|
| Sea $pCO_2$ | ProOceanus $CO_2$ Pro-CV | **± 3 ppm** | -5m (OO) |
| SST | CTD SBE16+ | **±0.005°C** | -5m (OO) |
| SSS | CTD SBE16+ | **±0.01 PSU** | -5m (OO) |
| Wind speed | Gill windsonic sensor | **±2%** | 10m (OO) |
| Wind speed | Vaisala WS425 | **±3%** | 60m (AO) |
| Atm. pressure | Vaisala BARO-1 | **±0.25 hPa** | 52m (AO) |
| Atm. $CO_2$ conc. | Picarro G2401 | **±0.1 ppm** | 57m (AO) |

- Ocean $pCO_2$, temperature and salinity are available at 5 m depth from October 2021 at OO
- Wind speed, atmospheric pressure, atmospheric $CO_2$ concentration are available at AO

$pCO_2$ issue with the a/d zero measurements between March and July 2022. An empirical correction was applied with an increased associated uncertainty.

# In situ $pCO_2$ and $CO_2$ fluxes

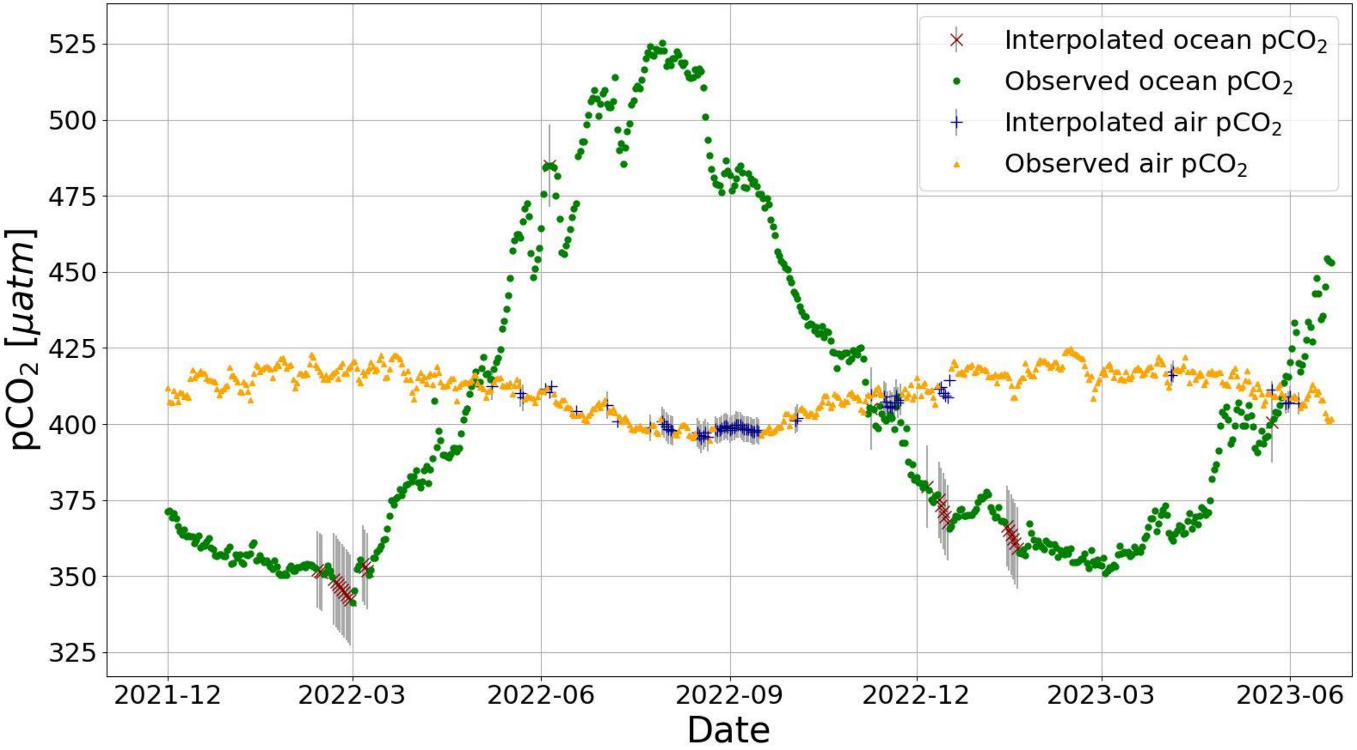


$pCO_2$ ATM
$pCO_2$ OCE

# In situ $pCO_2$ and $CO_2$ fluxes

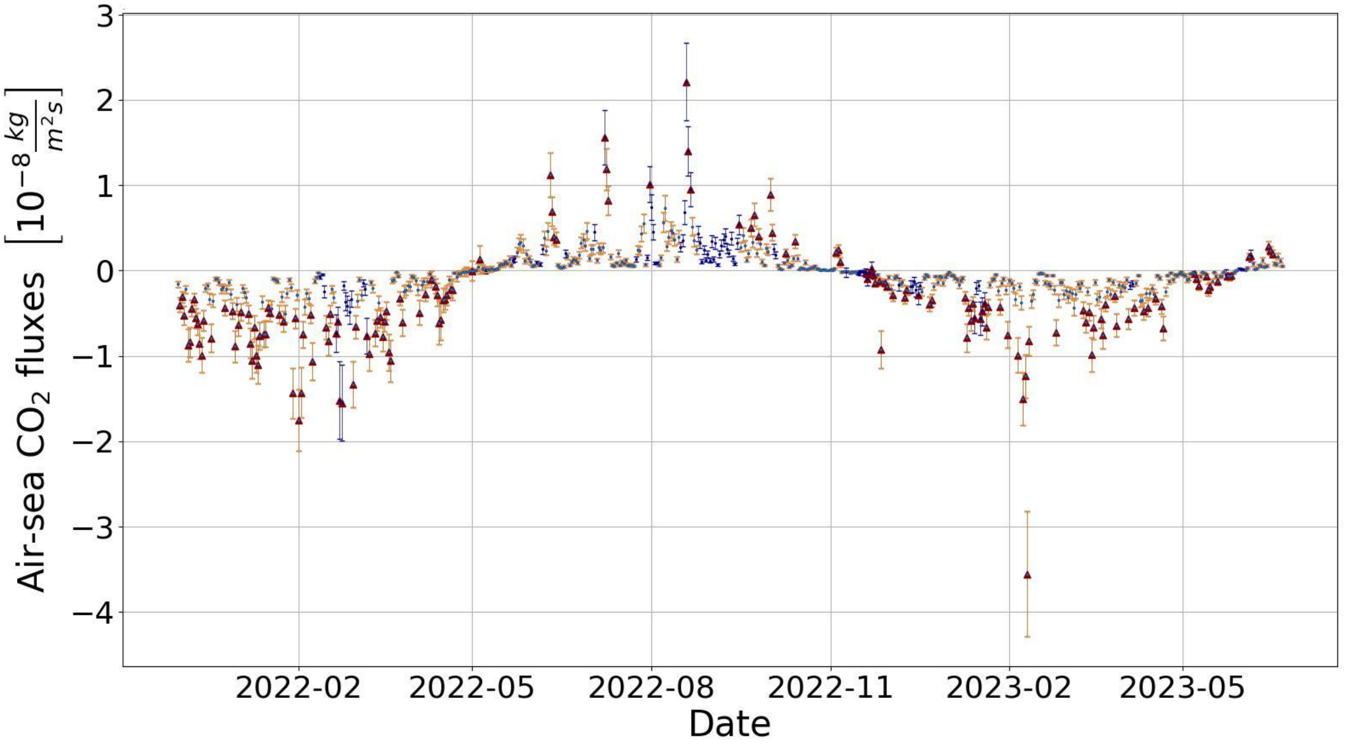


Observed
Interpolated
wspd > 8 m/s

# In situ $pCO_2$ and $CO_2$ fluxes

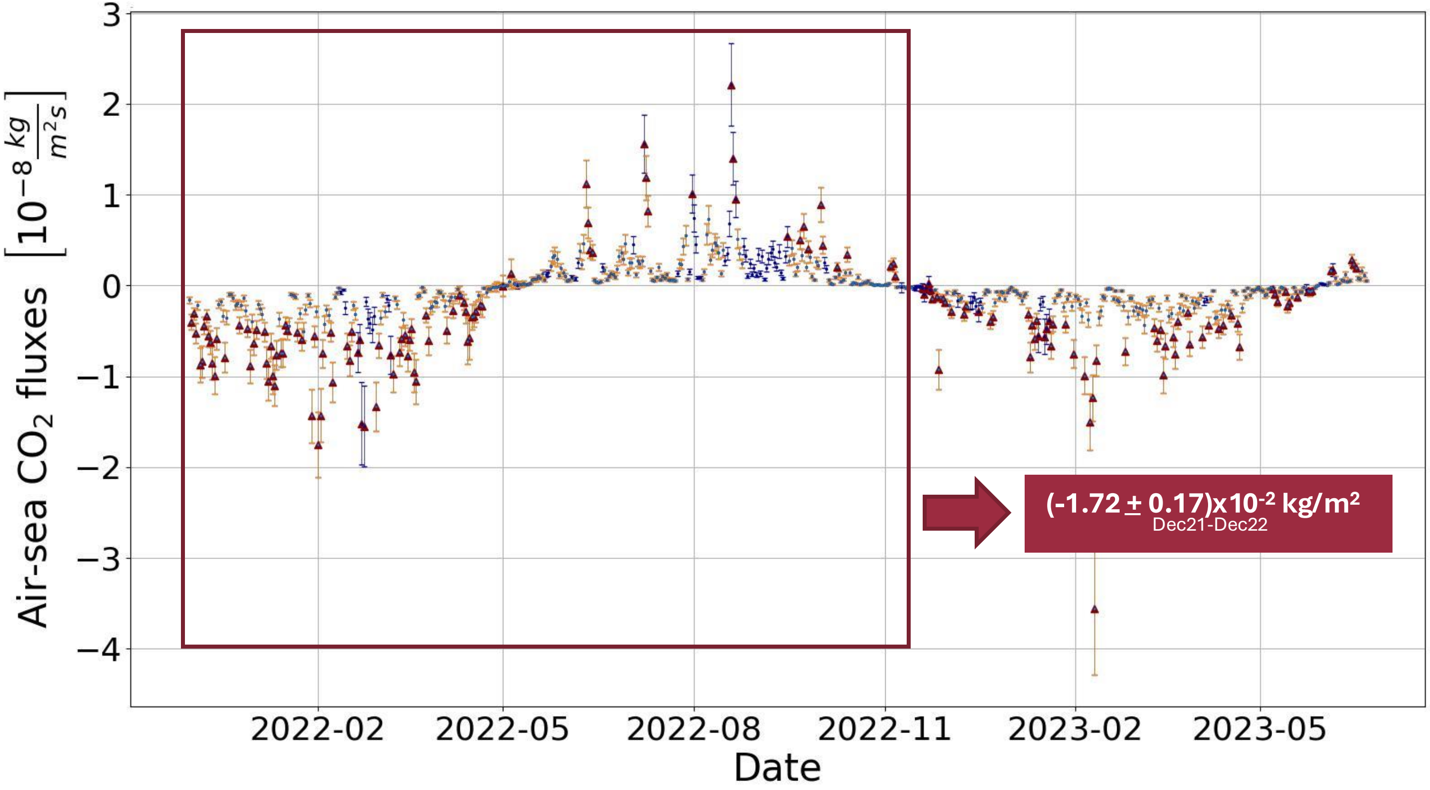


**$(-1.72 \pm 0.17)\times10^{-2}$ kg/m$^2$**
Dec21-Dec22

# In situ $pCO_2$ and $CO_2$ fluxes

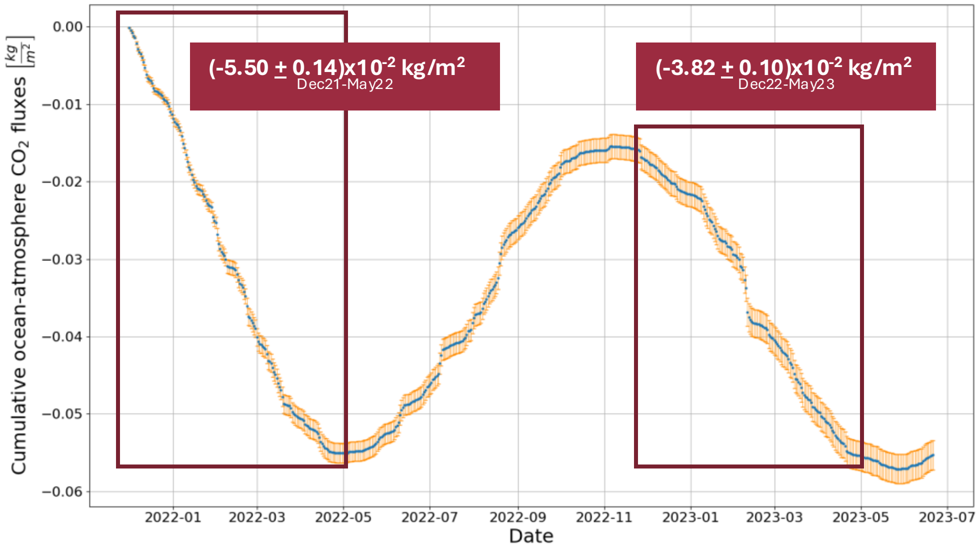


**Reduction of about 30% in ocean absorption**

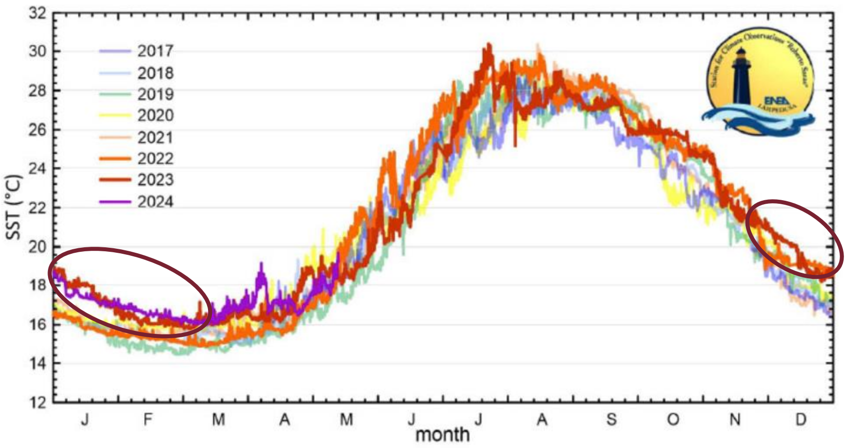


Hourly SST data; orange and red refers to 2022 and 2023

A. Mignot, K. von Schuckmann, P. Landschützer, F. Gasparin, S. van Gennip, C. Perruche, J. Lamouroux, and T. Amm. Decrease in air-sea $CO_2$ fluxes caused by persistent marine heatwaves. Nature Communications, 13(1):4300, 2022. doi: https://doi.org/10.1038/ s41467-022-31983-0.

# In situ $pCO_2$ and $CO_2$ fluxes

- Wind speed significantly influenced the development and persistence of the MHW in the Mediterranean Sea.
- Wind dynamics played a crucial role in reducing $CO_2$ exchange along the U.S. East Coast.
- A marked shift in wind speed distribution was observed at Lampedusa, with a notable reduction in moderate-to-high wind events.

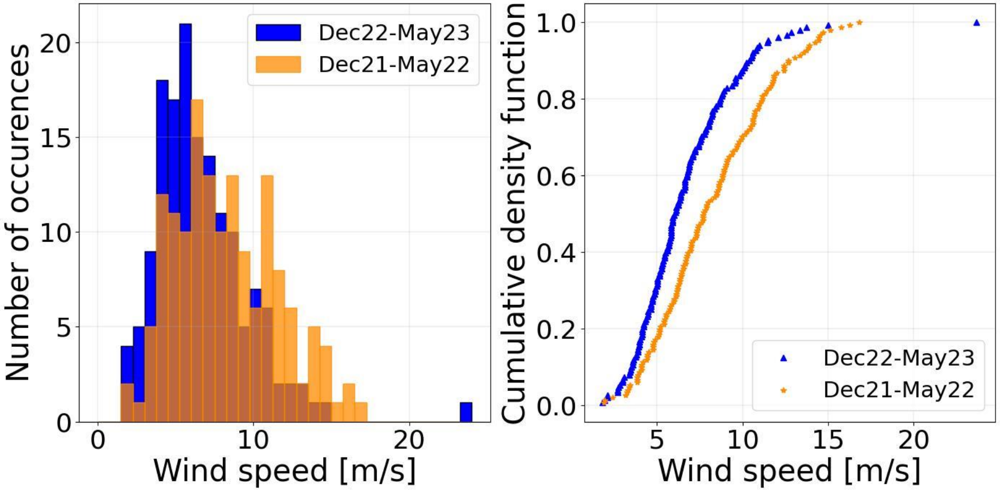


| | 2021-22 | 2022-23 |
|---|---|---|
| Days wind speed > 8 m/s | 71 | 42 |
| Days wind speed < 5 m/s | 26 | 47 |

Edwing, K., Wu, Z., Lu, W., Li, X., Cai, W.-J., & Yan, X.-H. (2024). Impact of marine heatwaves on air-sea $CO_2$ flux along the US East Coast. Geophysical Research Letters, 51 , e2023GL105363. doi: https://doi.org/10.1029/2023GL105363

# In situ $pCO_2$ and $CO_2$ fluxes

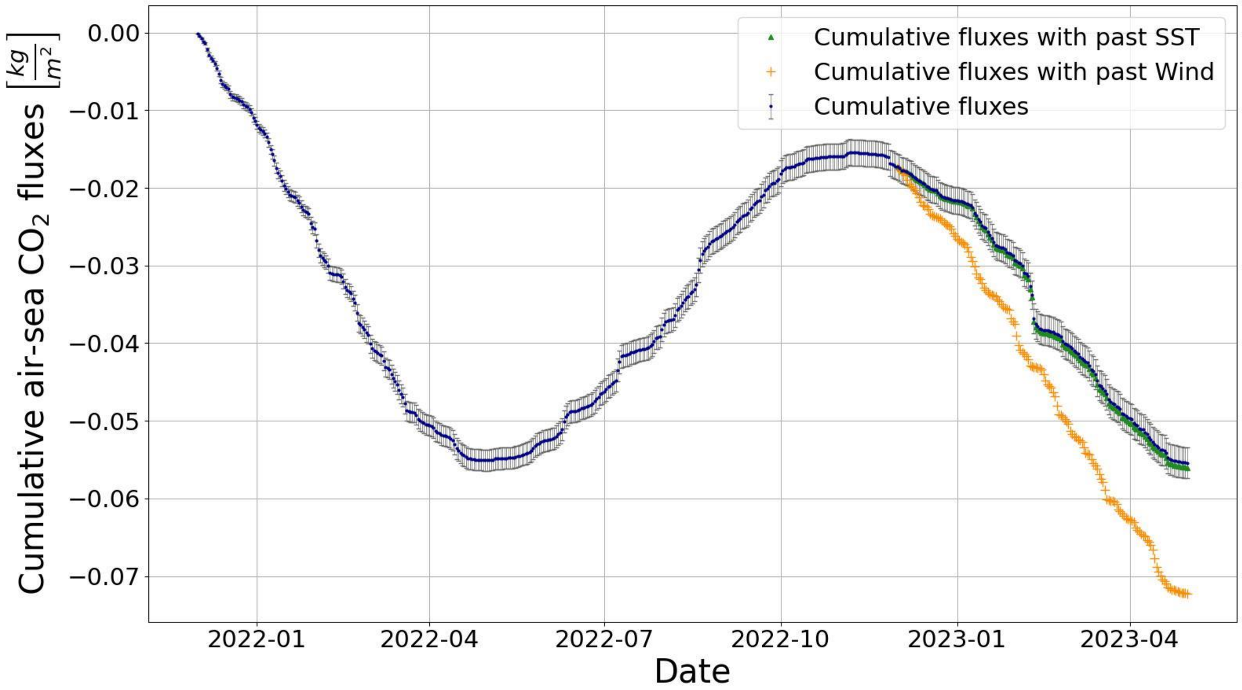


$(-3.82 \pm 0.10) \times 10^{-2}$ $kg/m^2$

$(-3.88 \pm 0.11) \times 10^{-2}$ $kg/m^2$

$(-5.50 \pm 0.14) \times 10^{-2}$ $kg/m^2$

Pecci et al., Large influence of the 2022-23 marine heatwave on the air-sea $CO_2$ flux in the Central Mediterranean, in submission *to Journal of Geophysical Research: Oceans*

# Outline:

- Carbon cycle
- Objectives
- In situ $pCO_2$ and $CO_2$ fluxes
- **Satellite algorithms**
- Results and discussion
- Conclusions and next steps

# Satellite algorithms

**Regional regression algorithms** are introduced to estimate $pCO_2$ with satellite measurable proxies:

| Variable | Dataset | Data type | Reference |
|---|---|---|---|
| **SST** | High Resolution and Ultra High-Resolution L3S SST | Satellite | CMEMS - Mediterranean Sea - High Resolution and Ultra High Resolution L3S Sea Surface Temperature. https://doi.org/10.48670/moi-00171 |
| **SSS** | Ocean Reanalysis System 5 (ORAS5) | Model | C3S - ORAS5 global ocean reanalysis monthly data from 1958 to present. *Copernicus Climate Change Service (C3S) Climate Data Store (CDS).* https://doi.org/10.24381/cds.67e8eeb7 |
| **Wind Speed** | Global Ocean Sea Surface Winds from Scatterometer | Satellite | CMEMS - Global Ocean Daily Gridded Sea Surface Winds from Scatterometer. Retrieved September 2023, from https://doi.org/10.48670/moi-00182 |
| **PAR** | OLCI – Sentinel-3 satellite | Satellite | Pecci, M. et al. (2024). Validation of photosynthetically active radiation by OLCI on Sentinel-3 against ground-based measurements in the central Mediterranean and possible aerosol effects. *European Journal of Remote Sensing, 57*(1). https://doi.org/10.1080/22797254.2024.2307617 |
| **PAR** | MODIS – Aqua satellite | Satellite | NASA Ocean Biology Processing Group - Aqua Daily Photosynthetically Active Radiation https://oceancolor.gsfc.nasa.gov/l3/ |
| **CHL** | Med. Sea, Bio-Geo-Chemical, Satellite Observations | Satellite | CMEMS - Mediterranean Sea, Bio-Geo-Chemical, L3, daily Satellite Observations (1997-ongoing) https://doi.org/10.48670/moi-00299 |
| Atm $xCO_2$ | In situ data-based fit | In situ-adapted | |
| Atmospheric pressure | ERA5 hourly reanalysis | Model | Hersbach, H., et al., (2023). ERA5 hourly data on single levels from 1940 to present. *Copernicus Climate Change Service (C3S) Climate Data Store (CDS).* https://doi.org/10.24381/cds.adbb2d47 |

# Satellite algorithms

**Traditional regression algorithms** to estimate $pCO_2$ with satellite measurable proxies:

- Use of least-squares method
- Use of different functional forms, including **multiple parameters and non-linear terms**
- Training and test on in situ **daily** datasets
- Use of **seasonal regression** to exploit the $pCO_2$ hysteresis
- Best performing models applied to satellite data

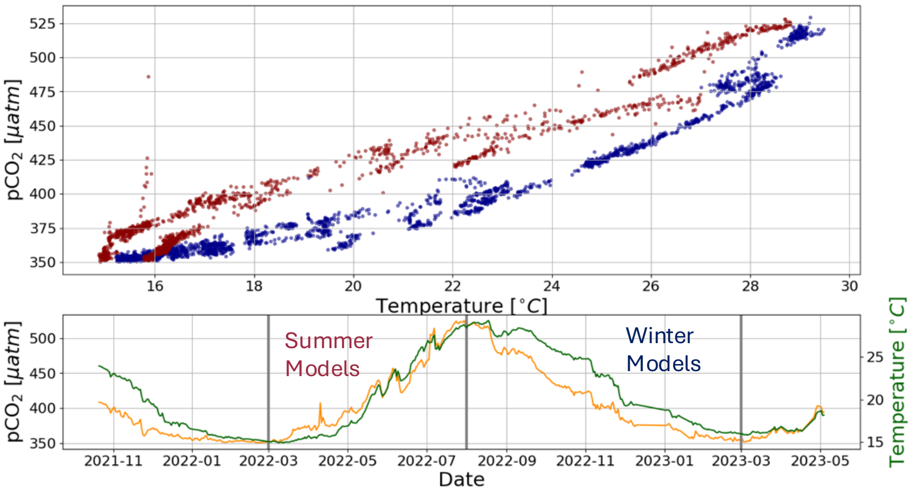

# Satellite algorithms

**Machine learning approach** to estimate $pCO_2$ with satellite measurable proxies:

- Use of eXtreme Gradient Boosting (**XGBoost**) algorithm
- Trained on **bi-hourly** data and tested on daily data
- Use of default and **cross-validated** settings
- Best performing models applied to satellite data

# Training and test set

The entire dataset spans from December 2021 to June 2023 (18 months):

- Single regression for the whole dataset («**Annual models**»)
    - Training set is composed of 12 months of data (Dec21 to Dec22)
    - Test set is composed of 6 months of data (Jan23-June23)

| Dataset | Bi-hourly | Daily |
|---|---|---|
| Training set | 2400 data pairs | 200 data pairs |
| Test set | / | 130 data pairs |

# Training and test set

- Traditional regression models divided to follow the branches of the hysteresis («**Seasonal models**»):
  - Summer models (Mar-Aug)
    - Training set: Mar22-Aug22
    - Test set: Mar23-Aug23
  - Winter models (Aug-Mar)
    - Training set: Dec21-Mar22 and Aug22-Dec22
    - Test set: Dec22-Mar23

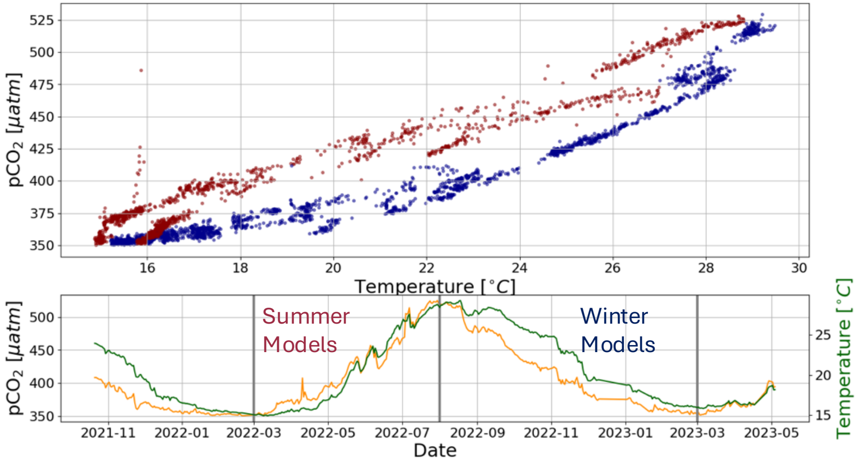


| Dataset | Summer models | Winter Models |
|---|---|---|
| Training set | 120 data pairs | 180 data pairs |
| Test set | 80 data pairs | 50 data pairs |

# Outline:

- Carbon cycle
- Objectives
- In situ $pCO_2$ and $CO_2$ fluxes
- Satellite algorithms
- **Results and discussion**
- Conclusions and next steps

# Traditional regression models

| Model | Functional Form | SST $[\frac{\mu atm}{°C}]$ | SST² $[\frac{\mu atm}{°C^2}]$ | SSS $[\frac{\mu atm}{PSU}]$ | CHL $[\frac{\mu atm \cdot L}{\mu g}]$ | PAR $[\frac{\mu atm \cdot m^2}{W}]$ | Wspd $[\frac{\mu atm \cdot s}{m}]$ | Const. $[\mu atm]$ |
|---|---|---|---|---|---|---|---|---|
| Mod4 | A·SST+B·SSS+C·CHL+ D·PAR+E | 9.20 | 0 | 10.35 | -99.12 | 0.13 | 0 | -146.36 |
| Mod6 | A·SST+B·CHL+C·PAR+ D·**wspd**+E | 9.23 | 0 | 0 | -98.99 | 0.11 | -0.66 | 247.17 |
| Mod9 | A·SST+B·CHL+C·PAR+D | 9.28 | 0 | 0 | -99.99 | 0.14 | 0 | 238.68 |
| Mod4_T2 | A·SST+B·**SST²** +C·SSS+D·CHL+E·PAR+F | 25.31 | -0.36 | 18.06 | -66.98 | 0.06 | 0 | -599.96 |
| Mod6_T2 | A·SST+B·**SST²**+C·CHL+ D·PAR+E·**wspd**+F | 24.56 | -0.34 | 0 | -68.94 | 0.05 | -0.78 | 90.43 |

Models functional form and coefficient for the «seasonal summer» models weighted with the reciprocal of the $pCO_2$ uncertainty

# Traditional regression models

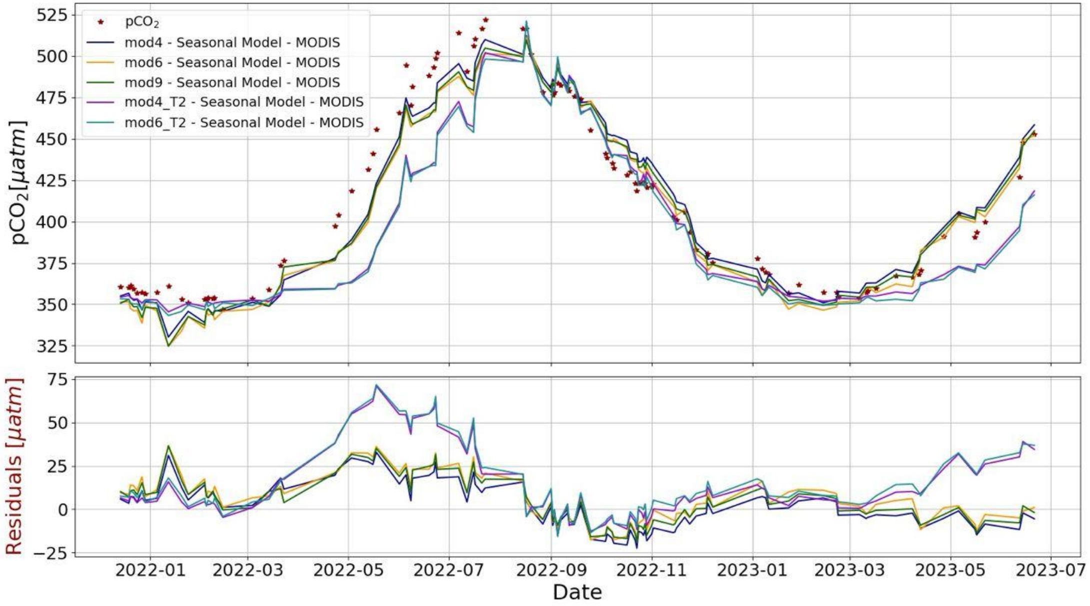


«Seasonal models» with MODIS PAR product non weighted regression

| | Model | $\bar{R}^2$ | RMSD [$\mu atm$] | Bias [$\mu atm$] |
|---|---|---|---|---|
| NW | **Mod4** | **0.94** | **13.1 (3%)** | **-1.5 ( < 1%)** |
| | Mod6 | 0.92 | 14.4 (3%) | -5.8 (2%) |
| | **Mod9** | **0.93** | **13.7 (3%)** | **-4.3 (1%)** |
| | Mod4_T2 | 0.75 | 24.1 (6%) | -13.1 (3%) |
| | Mod6_T2 | 0.74 | 25.1 (6%) | -14.8 (3%) |
| W | **Mod4** | **0.93** | **13.2 (3%)** | **-1.2 (< 1%)** |
| | Mod6 | 0.92 | 14.6 (3%) | -5.9 (2%) |
| | Mod9 | 0.92 | 14.0 (3%) | -4.0 (1%) |
| | Mod4_T2 | 0.72 | 25.0 (6%) | -13.4 (3%) |
| | Mod6_T2 | 0.71 | 26.1 (6%) | -15.5 (3%) |

# Traditional regression models

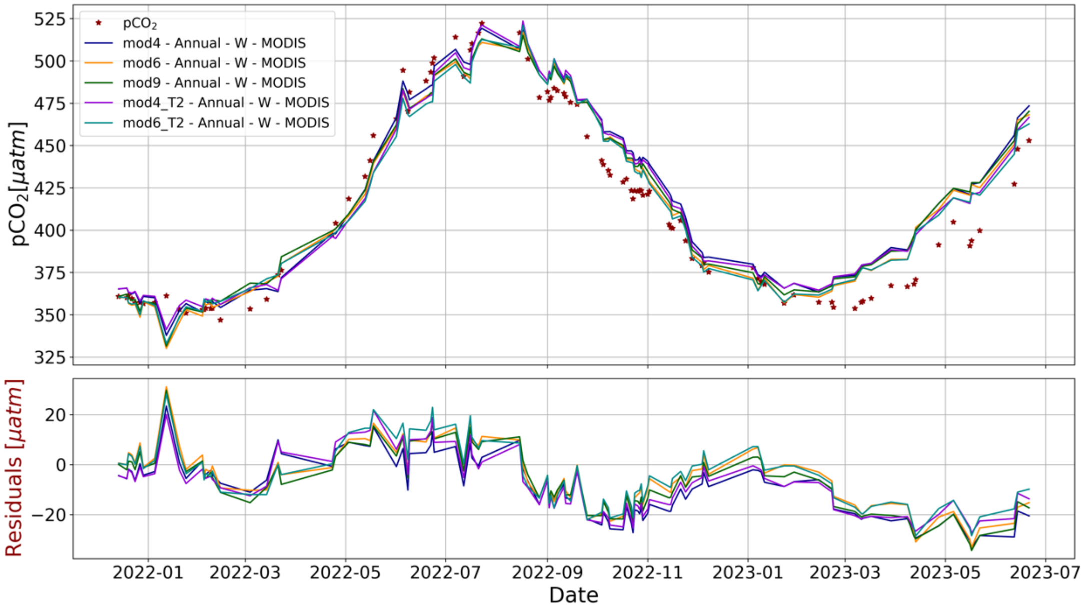


«Annual models» with MODIS PAR product weighted regression

| | Model | $\bar{R}^2$ | RMSD $[\mu atm]$ | Bias $[\mu atm]$ |
|---|---|---|---|---|
| NW | Mod4 | 0.81 | 21.2 (5%) | 17.2 (4%) |
| | Mod6 | 0.82 | 20.1 (5%) | 15.0 (3%) |
| | Mod9 | 0.81 | 20.7 (5%) | 15.8 (4%) |
| | Mod4_T2 | 0.81 | 21.2 (5%) | 17.2 (4%) |
| | Mod6_T2 | 0.83 | 20.1 (5%) | 15.0 (3%) |
| W | Mod4 | 0.91 | 14.9 (3%) | 9.2 (2%) |
| | **Mod6** | **0.93** | **13.2 (3%)** | **5.3 (1%)** |
| | Mod9 | 0.92 | 13.9 (3%) | 6.8 (2%) |
| | Mod4_T2 | 0.92 | 14.2 (3%) | 7.9 (2%) |
| | **Mod6_T2** | **0.94** | **13.0 (3%)** | **4.4 (1%)** |

# ML models

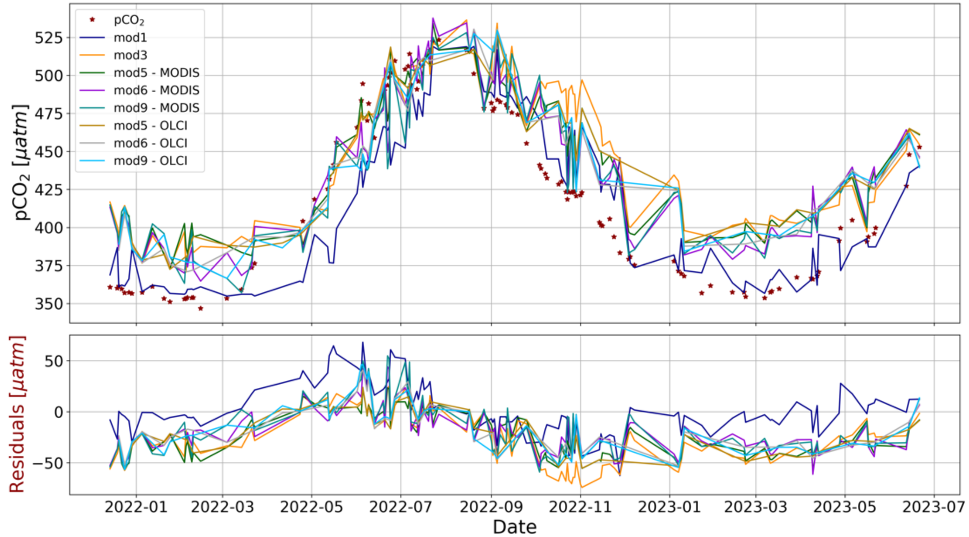


| Model | Input variables |
|---|---|
| Mod1 | SST |
| Mod3 | SST, SSS, CHL |
| Mod5 | SST, SSS, CHL, PAR, WSPD |
| Mod6 | SST, CHL, PAR, WSPD |
| Mod9 | T, CHL, PAR |

| | Model | $\overline{R}^2$ | RMSD $[\mu atm]$ | Bias $[\mu atm]$ |
|---|---|---|---|---|
| **D** | **Mod1** | **0.76** | **25.0 (6%)** | **-1.4 (< 1%)** |
| | **Mod3** | 0.30 | 37.0 (8%) | 26.1 (6%) |
| | **Mod5** | 0.33 | 34.2 (8%) | 24.3 (5%) |
| | **Mod6** | **0.51** | **31.4 (7%)** | **18.8 (4%)** |
| | **Mod9** | 0.49 | 32.4 (7%) | 19.9 (4%) |
| **CV** | **Mod1** | **0.76** | **25.0 (6%)** | **-1.7 (<1%)** |
| | **Mod3** | 0.35 | 37.4 (8%) | 27.1 (6%) |
| | **Mod5** | 0.48 | 31.4 (7%) | 23.5 (5%) |
| | **Mod6** | **0.61** | **28.7 (7%)** | **18.4 (4%)** |
| | **Mod9** | 0.54 | 31.3 (7%) | 17.9 (4%) |

# Performance summary

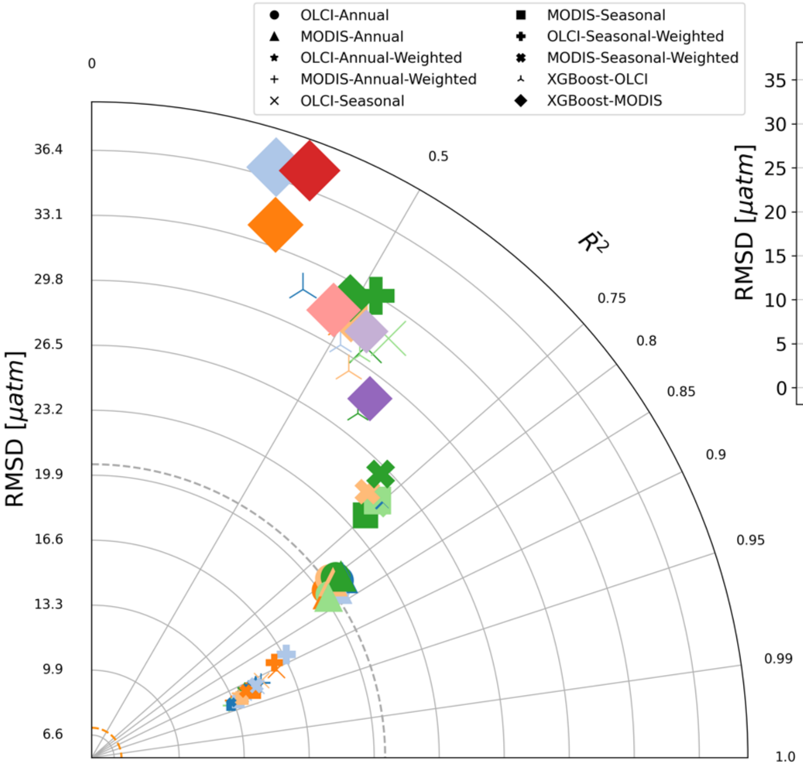


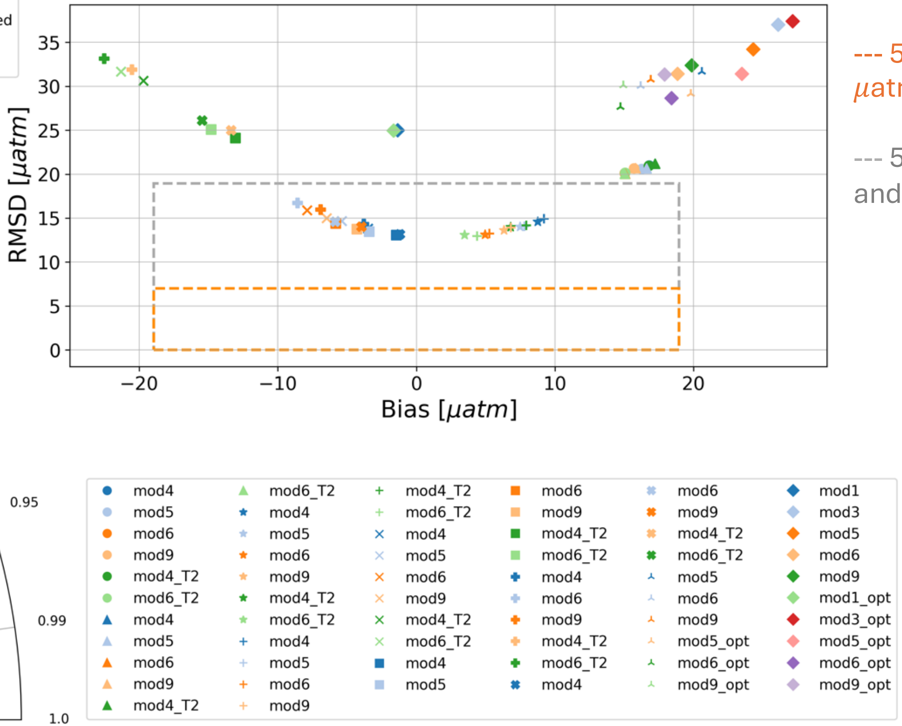


--- 5% bias, 7 $\mu$atm RMSD

--- 5% bias and RMSD

# Fluxes estimates

- Fluxes computed using satellite-estimated $pCO_2$ and satellite/model-based ancillary quantities

- The need of simultaneous data from different dataset leads to a reduced dataset (approximately 100 data pairs for the MODIS-based dataset and 50 for the OLCI-based dataset)

| | Model | $R^2$ | RMSD $[\frac{kg}{m^2s}]$ | Bias $[\frac{kg}{m^2s}]$ |
|---|---|---|---|---|
| **O** | **Mod6** | 0.74 | $1.2 \cdot 10^{-9}$ (100%) | $-2.1 \cdot 10^{-10}$ (18%) |
| | **Mod4_T2** | 0.74 | $1.2 \cdot 10^{-9}$ (100%) | $-2.4 \cdot 10^{-10}$ (20%) |
| | **Mod5_XGBoost** | 0.57 | $1.6 \cdot 10^{-9}$ (140%) | $-6.0 \cdot 10^{-10}$ (50%) |
| | **Mod9_XGBoost** | 0.56 | $1.6 \cdot 10^{-9}$ (140%) | $-5.3 \cdot 10^{-10}$ (47%) |
| **M** | **Mod4** | 0.75 | $1.3 \cdot 10^{-9}$ (110%) | $-8.1 \cdot 10^{-11}$ (7%) |
| | **Mod9** | **0.75** | **$1.3 \cdot 10^{-9}$ (110%)** | **$1.0 \cdot 10^{-12}$ (<< 1%)** |
| | **Mod6_T2** | 0.71 | $1.4 \cdot 10^{-9}$ (120%) | $-3.0 \cdot 10^{-10}$ (25%) |
| | **Mod1_XGBoost** | 0.64 | $1.5 \cdot 10^{-9}$ (130%) | $-3.0 \cdot 10^{-10}$ (25%) |
| | **Mod3_XGBoost** | 0.24 | $2.2 \cdot 10^{-9}$ (190%) | $-1.2 \cdot 10^{-9}$ (10%) |
| | **Mod6_XGBoost** | 0.37 | $2.0 \cdot 10^{-9}$ (185%) | $-9.0 \cdot 10^{-10}$ (80%) |

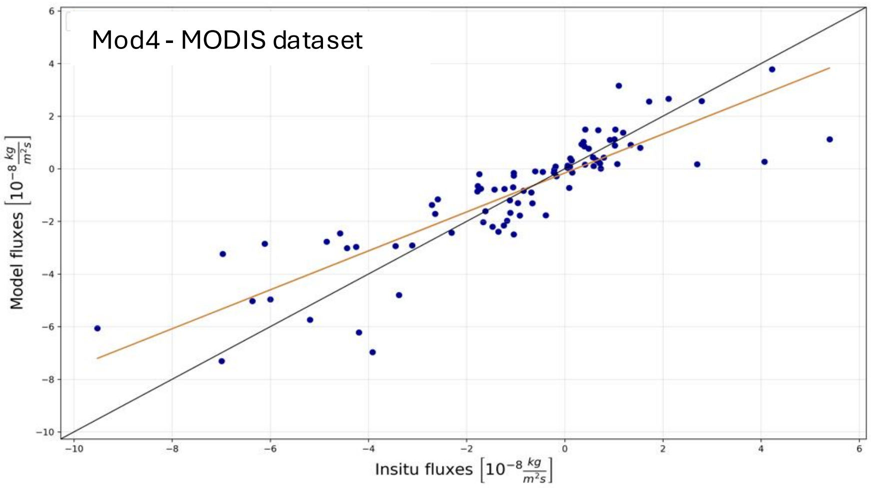

# Outline:

- Carbon cycle
- Objectives
- In situ $pCO_2$ and $CO_2$ fluxes
- Satellite algorithms
- Results and discussion
- **Conclusions and next steps**

# Conclusion and next steps

- Observed data of $pCO_2$ and $CO_2$ fluxes show a net sink effect

- Strong MHW impact on the magnitude of the exchanges

- The use of regional regression algorithms improve the agreement between estimated and observed $pCO_2$ values (with traditional regressions performing better than ML, probably due to the small dataset)

- $CO_2$ fluxes estimates using satellite-based $pCO_2$ and ancillary quantities show a good agreement with fluxes computed using observed data

| **Dataset** | **Bias** | **RMSD** | **$R^2$** |
|---|---|---|---|
| CMEMS $pCO_2$ | 28.4 $[\mu atm]$ (7%) | 40.0 $[\mu atm]$ (10%) | 0.91 |
| MPNR algorithm | -7.4 $[\mu atm]$ (2%) | 31.9 $[\mu atm]$ (7%) | 0.59 |
| **Mod6_T2** | **4.4 $[\mu atm]$ (1%)** | **13.0 $[\mu atm]$ (3%)** | **0.94** |
| CMEMS Fluxes | $9.8 \cdot 10^{-10}$ $[\frac{kg}{m^2 s}]$ (86%) | $3.1 \cdot 10^{-9}$ $[\frac{kg}{m^2 s}]$ (270%) | 0.22 |
| **Mod9** | **$1.0 \cdot 10^{-12}$ $[\frac{kg}{m^2 s}]$ (<< 1%)** | **$1.3 \cdot 10^{-9}$ $[\frac{kg}{m^2 s}]$ (110%)** | **0.75** |

# Conclusion and next steps

- Despite being promising, a larger dataset is needed for a more robust statistics:
    - Use of different satellite input (CMEMS L4 salinity, ERA5 or CCMP wind speed, SEVIRI daily PAR) to increase the dataset size for $pCO_2$ and fluxes estimates
- Carry on the monitoring with a special focus on the SST and MHW impact on ocean absorption efficiency
- Extend the $pCO_2$ and $CO_2$ fluxes estimates to a broader area
- Compare the estimates with other Mediterranean carbon datasets (e.g., Integrated Carbon Observation System stations)

# Thanks for the attention!

# Performance metrics

Bias = $\frac{1}{N}\sum_i (y_i - x_i)$

RMSD = $\sqrt{\frac{1}{N}\sum_i (y_i - x_i)^2}$

$$\mathrm{R}^2 = 1 - \frac{\sum_i (y_i - x_i)^2}{\sum_i (y_i - \bar{y})^2}$$

$$\bar{R}^2 = 1 - (1 - \mathrm{R}^2)\frac{n-1}{n-k-1}$$

Where

- y is the predicted values
- x is the observed value
- n is the dataset size
- k is the number of parameters used in the regression

# $pCO_2$ hysteresis

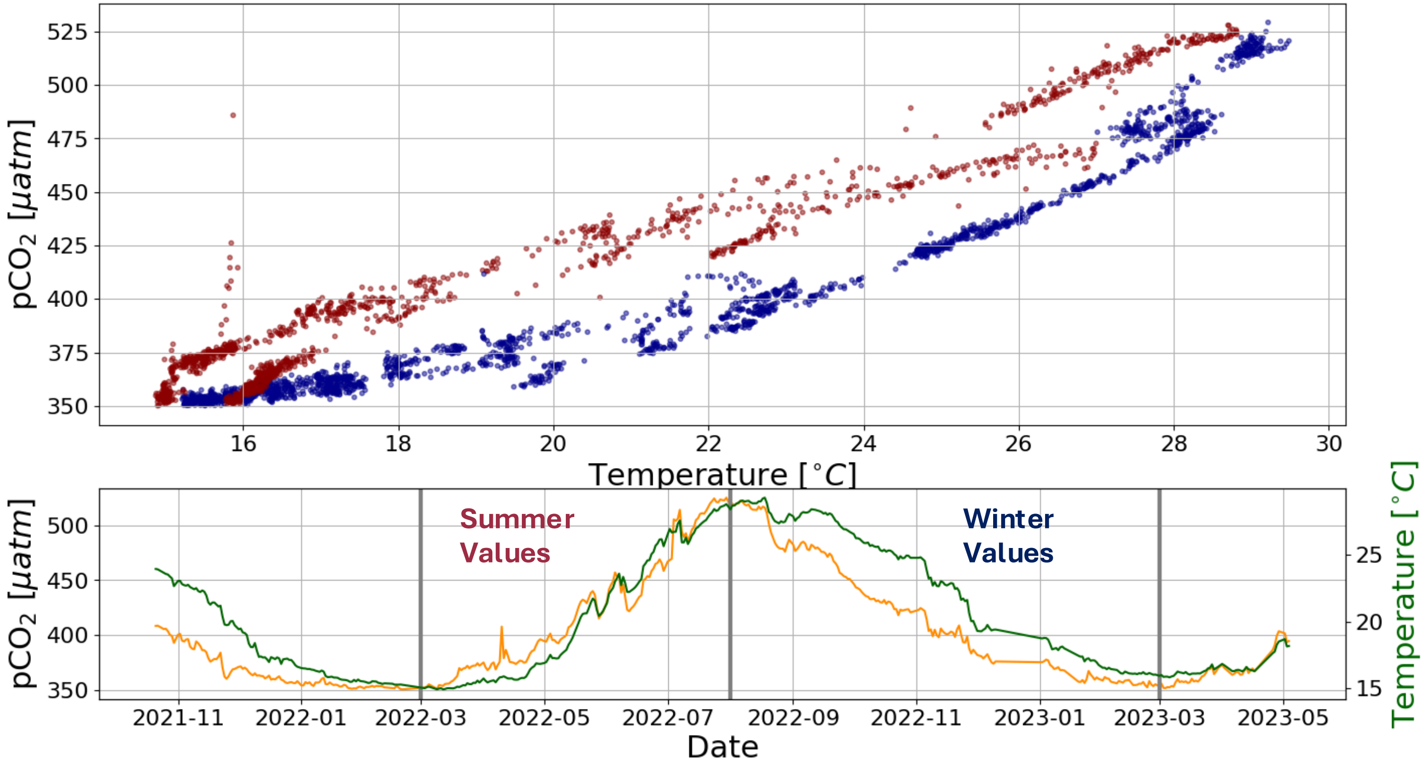

# Marine carbon cycle

- Current monitoring mainly rely on model-based estimates of $pCO_2$ and $CO_2$ fluxes

| Dataset | Bias | RMSD | $R^2$ |
|---|---|---|---|
| CMEMS $pCO_2$ | 28.4 $[\mu atm]$ (7%) | 40.0 $[\mu atm]$ (10%) | 0.91 |
| CMEMS Fluxes | $9.8 \cdot 10^{-10}$ $[\frac{kg}{m^2 s}]$ (86%) | $3.1 \cdot 10^{-9}$ $[\frac{kg}{m^2 s}]$ (280%) | 0.22 |

## $pCO_2$

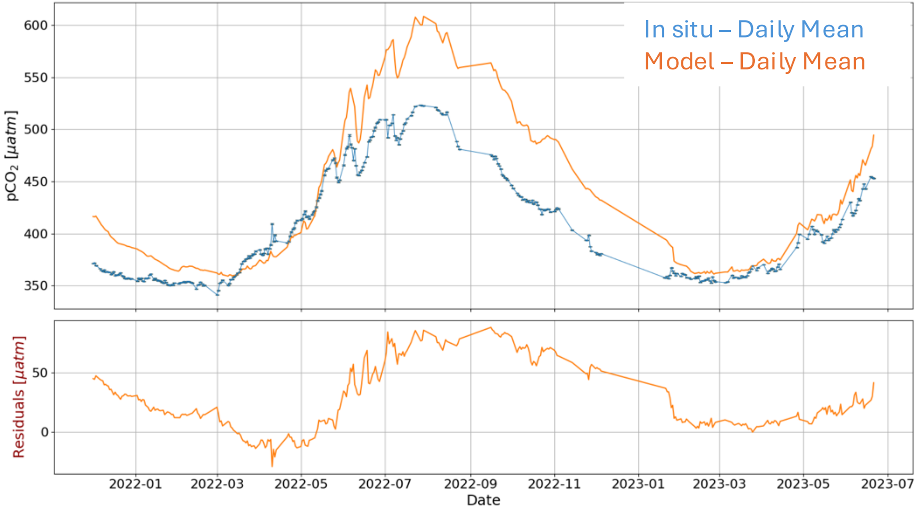


## $CO_2$ Fluxes

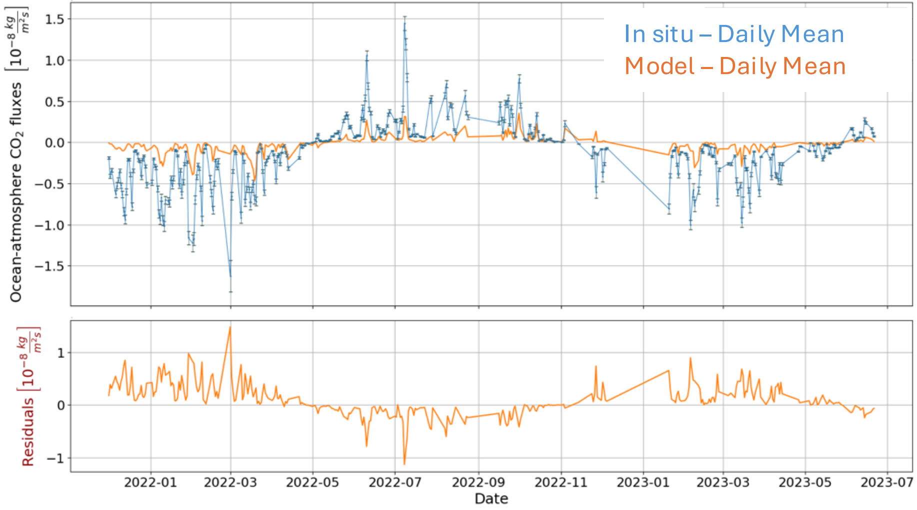


Mediterranean Sea Biogeochemistry Analysis and Forecast - https://doi.org/10.25423/cmcc/medsea_analysisforecast_bgc_006_014_medbfm3

# Marine carbon cycle

- Current monitoring mainly rely on model-based estimates of $pCO_2$ and $CO_2$ fluxes

- Works on satellite-based estimates of $pCO_2$

| Dataset | Bias | RMSD | $R^2$ |
|---|---|---|---|
| MPNR algorithm global data | / | 5.35-8.77 $[\mu atm]$ | 0.82-0.93 |
| MPNR algorithm on Med | -7.4 $[\mu atm]$ (2%) | 31.9 $[\mu atm]$ (8%) | 0.59 |

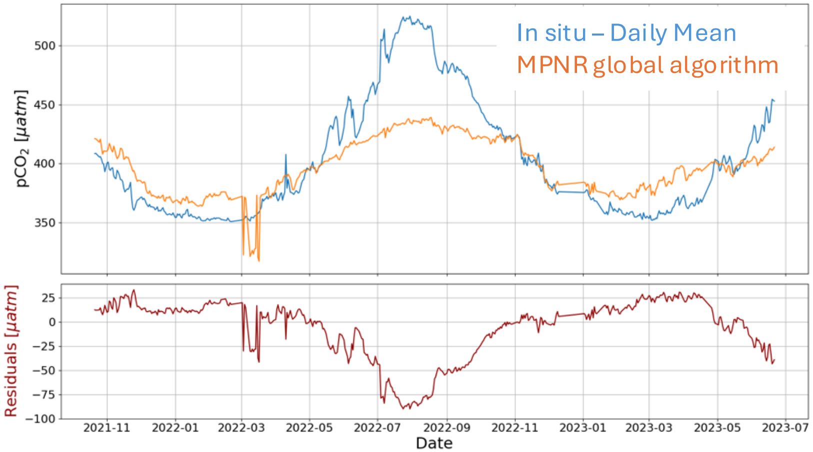


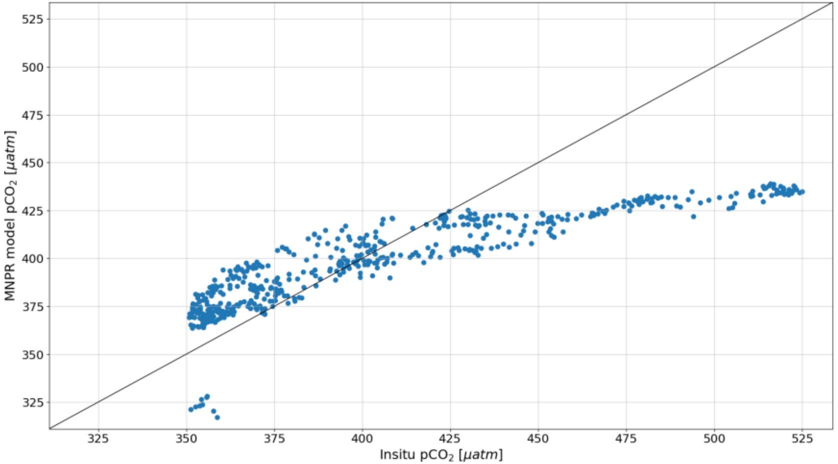


K. V. Krishna, P. Shanmugam and P. V. Nagamani, "A Multiparametric Nonlinear Regression Approach for the Estimation of Global Surface Ocean pCO2 Using Satellite Oceanographic Data," in *IEEE Journal of Selected Topics in Applied Earth Observations and Remote Sensing*, vol. 13, pp. 6220-6235, 2020, doi: 10.1109/JSTARS.2020.3026363.